

Kinetic Study and Reactivity Trends of Hydroxide Ion Attack on Some Chromen-2-one Laser Dyes in Binary Water–Methanol and Water–Acetone Mixtures¹

E. A. Abu-Gharib, R. M. El-Khatib, L. A. E. Nassr, and A. M. Abu-Dief

Chemistry Department, Faculty of Science, Sohag University, Sohag, 82534 Egypt
fax: +20934601159; e-mail: ahmed_benzoic@yahoo.com

Received January 16, 2014

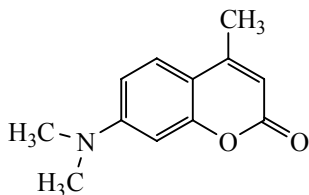
Abstract—The kinetics of base-catalyzed hydrolysis of 7-dimethylamino-4-methyl-2*H*-chromen-2-one (DMAC) and 7-diethylamino-4-methyl-2*H*-chromen-2-one (DEAC) in binary water–methanol and water–acetone mixtures were studied in the temperature range from 288 to 313 K. The activation and thermodynamic parameters of these reactions were evaluated and discussed. The change in the activation energy in going from water to aqueous methanol and aqueous acetone was estimated from the kinetic data. Base-catalyzed hydrolysis of DMAC and DEAC in aqueous methanol and aqueous acetone follows the first-order kinetic law with respect to hydroxide ion, $k_{\text{obs}} = k_2[\text{OH}^-]$. The hydrolysis rate constants of DMAC and DEAC decrease as the fraction of methanol or acetone in the binary mixture rises, which is due to destabilization of OH^- ion. The high negative entropies of activation support the proposed mechanism involving formation of an intermediate complex and reflect rigidity and stability of the latter. Opening of the pyran ring in the intermediate complex is the rate-determining step.

DOI: 10.1134/S1070363214030293

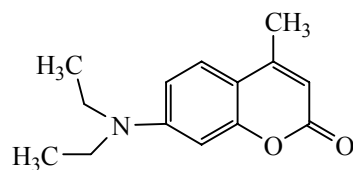
Chromen-2-ones are ubiquitous in nature. They have been extensively studied due to their practical applications [1]. Chromen-2-ones have such marked physiological effects as active hypotoxicity, carcinogenicity, anticoagulant action, and antibiotic and anti-inflammatory activity [2–6]; they are also used as biological and chemical sensors, fluorescent probes, and laser dyes [7–9]. Chromen-2-ones containing an electron-donating group in the 7-position and a heterocyclic electron-acceptor residue in the 3-position are recognized as fluorescent dyes suitable for application to synthetic fibers [10]. Chromen-2-ones have a wide variety of uses in industry, mainly due to their strong fragrant odor [11, 12]. Their uses also include that of a sweetener and fixative of perfumes, an enhancer of natural oils, such as lavender, a food additive in

combination with vanillin, a flavor/odor stabilizer in tobaccos, an odor masker in paints and rubbers, and, finally, they are used in electroplating to reduce the porosity and increase the brightness of various deposits, such as nickel [13]. 7-Dimethylamino- and 7-diethylamino-4-methyl-2*H*-chromen-2-ones are used as laser dyes for the blue–green region [9, 14, 15] and as indicator dyes [16].

In continuation of our work [17], we report here the effects of methanol and acetone as co-organic solvents on the kinetics of base-catalyzed hydrolysis of 7-dimethylamino-4-methyl-2*H*-chromen-2-one (DMAC) and 7-diethylamino-4-methyl-2*H*-chromen-2-one (DEAC) at different temperatures to gain more information about the activation parameters of these reactions.



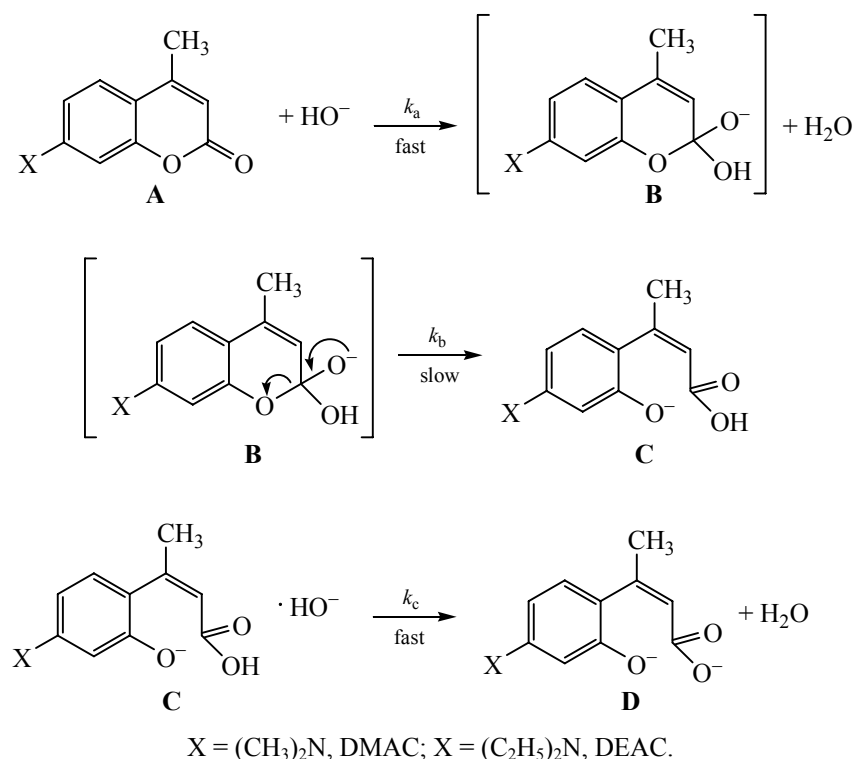
7-Dimethylamino-4-methyl-2*H*-chromen-2-one
methyl-2*H*-chromen-2-one (DMAC)



7-Diethylamino-4-methyl-2*H*-chromen-2-one
(DEAC)

¹ The text was submitted by the authors in English.

Scheme 1.



The absorption bands in the electronic spectra of DMAC and DEAC at λ_{\max} 373 and 383 nm, respectively, can be ascribed to $n\text{-}\pi^*$ transition involving the lone electron pair on the nitrogen atom in position 7. In acid medium these bands disappear because of protonation [18].

It can be realized from the repeated spectral scans (Fig. 1) that the effect of NaOH on DMAC and DEAC leads to opening of the pyranone ring as the rate-determining stage with formation of (2Z)-3-(4-dimethylamino-2-hydroxyphenyl)but-2-enoic and (2Z)-3-(4-diethylamino-2-hydroxyphenyl)but-2-enoic acid salts, respectively, as shown in Scheme 1 [17, 19]. The hydrolysis products absorb at λ 300 nm for DMAC and λ 310 nm for DEAC.

The observed first-order rate constants k_{obs} as a function of $[\text{OH}^-]$ at different water–methanol and water–acetone ratios and k_2 values calculated from the $k_{\text{obs}}\text{--}[\text{OH}^-]$ plots by the least squares method using Microcal Origin 7.5 are given in Tables 1 and 2; the error in their determination did not exceed 2%. The k_{obs} values appreciably decrease as the fraction of the organic solvent in water–methanol and water–acetone mixtures increases. This trend can be attributed to the increase in transfer chemical potential for hydrophilic

hydroxide ion, $\delta_{\text{m}}\mu^0(\text{OH}^-)$ as the solvent becomes less aqueous [20]. The effect of the organic solvent on base-catalyzed hydrolysis of DMAC and DEAC is stronger than that of OH^- ion concentration (Figs. 2, 3), which may be ascribed to the salting out of OH^- ions.

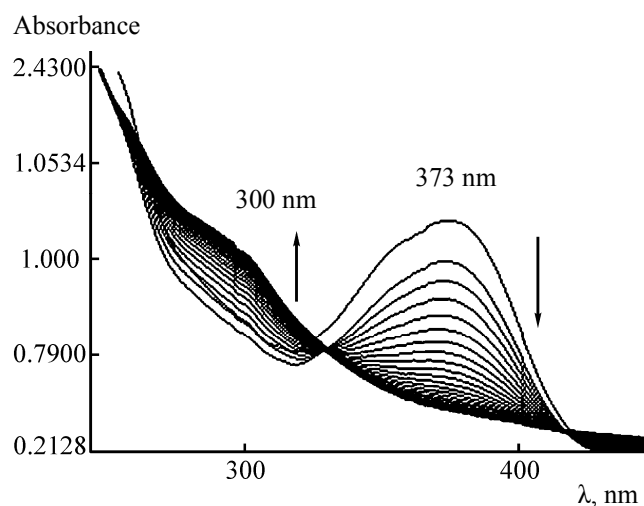


Fig. 1. Repeated spectral scans of DMAC at $[\text{OH}^-] = 0.35 \text{ M}$, $[\text{DMAC}] = 1 \times 10^{-3} \text{ M}$, $I = 0.5 \text{ M}$; 298 K, time interval 2 min.

Table 1. Second-order rate constants and activation parameters for the base hydrolysis of DMAC and DEAC in binary water–methanol mixtures at different temperatures ($I = 0.5$ M)

| MeOH, vol % | 283 K | 288 K | 293 K | 298 K | 303 K | 308 K | 313 K | E_a , kJ/mol | ΔH^\ddagger , kJ/mol | ΔG^\ddagger , kJ/mol | ΔS^\ddagger , J mol ⁻¹ K ⁻¹ | A , L mol ⁻¹ s ⁻¹ |
|----------------|---|-------|-------|-------|-------|-------|-------|-------------------|---------------------------------|---------------------------------|--|--|
| DMAC | $k_2 \times 10^4$, L mol ⁻¹ s ⁻¹ | | | | | | | | | | | |
| 0 | 2.88 | 3.80 | 5.80 | 7.79 | — | — | — | 46.15 | 43.65 | 71.22 | –92.50 | 3.11×10^5 |
| 10 | 2.31 | 2.91 | 4.59 | 5.84 | 9.18 | — | — | 47.20 | 44.74 | 71.60 | –90.10 | 1.15×10^5 |
| 20 | 1.91 | 2.32 | 3.81 | 4.54 | 7.70 | 9.83 | — | 48.93 | 46.48 | 72.62 | –87.70 | 7.90×10^5 |
| 40 | 1.12 | 1.38 | 2.28 | 2.76 | 4.45 | 5.79 | 9.40 | 51.61 | 49.17 | 74.00 | –83.40 | 5.45×10^4 |
| 50 | 0.81 | 1.18 | 1.63 | 2.38 | 3.50 | 4.65 | 7.50 | 52.91 | 50.46 | 74.66 | –81.20 | 1.76×10^4 |
| 60 | 0.67 | 0.95 | 1.35 | 1.90 | 2.71 | 3.69 | 5.61 | 54.30 | 51.85 | 75.30 | –78.70 | 7.97×10^3 |
| DEAC | $k_2 \times 10^3$, L mol ⁻¹ s ⁻¹ | | | | | | | | | | | |
| 0 | 1.47 | 1.94 | 2.91 | 3.99 | 5.93 | 7.95 | — | 50.12 | 47.62 | 74.60 | –90.40 | 1.00×10^5 |
| 10 | 1.17 | 1.45 | 2.33 | 2.92 | 4.56 | 5.85 | 9.39 | 51.31 | 48.87 | 75.10 | –88.00 | 7.65×10^4 |
| 20 | 0.92 | 1.20 | 1.90 | 2.40 | 3.90 | 4.81 | 8.00 | 52.95 | 50.52 | 76.00 | –85.60 | 4.25×10^4 |
| 40 | 0.55 | 0.86 | 1.10 | 1.73 | 2.28 | 3.44 | 4.74 | 55.75 | 53.31 | 77.54 | –81.30 | 7.65×10^3 |
| 50 | 0.44 | 0.72 | 0.88 | 1.49 | 1.71 | 2.97 | 3.60 | 57.10 | 54.64 | 78.20 | –79.00 | 5.20×10^3 |
| 60 | 0.34 | 0.57 | 0.67 | 1.16 | 1.33 | 2.25 | 2.60 | 58.6 | 56.17 | 79.00 | –76.50 | 3.82×10^3 |

Table 2. Second-order rate constants and activation parameters for the base hydrolysis of DMAC and DEAC in binary water–acetone mixtures at different temperatures ($I = 0.5$ M)

| Acetone, vol % | 283 K | 288 K | 293 K | 298 K | 303 K | 308 K | 313 K | E_a , kJ/mol | ΔH^\ddagger , kJ/mol | ΔG^\ddagger , kJ/mol | ΔS^\ddagger , J mol ⁻¹ K ⁻¹ | A , L mol ⁻¹ s ⁻¹ |
|-------------------|---|-------|-------|-------|-------|-------|-------|-------------------|---------------------------------|---------------------------------|--|--|
| DMAC | $k_2 \times 10^3$, L mol ⁻¹ s ⁻¹ | | | | | | | | | | | |
| 0 | 2.91 | 3.73 | 5.85 | 7.58 | — | — | — | 44.70 | 42.19 | 72.00 | –95.10 | 8.90×10^5 |
| 10 | 2.64 | 3.35 | 5.20 | 6.90 | 10.43 | — | — | 45.35 | 43.23 | 72.31 | –92.50 | 7.47×10^5 |
| 20 | 2.40 | 2.60 | 4.26 | 5.26 | 8.27 | 10.60 | — | 46.85 | 44.41 | 73.43 | –90.40 | 5.25×10^5 |
| 40 | 1.51 | 1.86 | 2.96 | 3.68 | 5.90 | 7.50 | 11.61 | 48.71 | 46.57 | 74.74 | –85.80 | 1.20×10^5 |
| 50 | 1.21 | 1.50 | 2.40 | 3.08 | 4.83 | 6.31 | 9.60 | 49.45 | 47.61 | 75.37 | –83.60 | 8.55×10^4 |
| 60 | 0.88 | 1.35 | 1.79 | 2.66 | 3.52 | 5.00 | 7.31 | 50.64 | 48.75 | 76.00 | –81.10 | 6.80×10^4 |
| DEAC | $k_2 \times 10^3$, L mol ⁻¹ s ⁻¹ | | | | | | | | | | | |
| 0 | 1.46 | 1.89 | 2.90 | 3.95 | 5.85 | — | — | 48.75 | 46.25 | 73.90 | –92.80 | 2.29×10^5 |
| 10 | 1.32 | 1.70 | 2.60 | 3.37 | 5.25 | 6.80 | — | 49.35 | 47.31 | 74.30 | –90.60 | 1.27×10^5 |
| 20 | 1.13 | 1.42 | 2.24 | 2.81 | 4.44 | 5.55 | 9.11 | 50.65 | 48.25 | 74.44 | –87.90 | 1×10^5 |
| 40 | 0.94 | 1.14 | 1.90 | 2.30 | 3.75 | 4.54 | 7.60 | 52.71 | 50.26 | 75.23 | –83.80 | 6.89×10^4 |
| 50 | 0.75 | 0.95 | 1.50 | 1.92 | 3.05 | 3.80 | 6.00 | 53.65 | 51.37 | 75.63 | –81.40 | 3.28×10^4 |
| 60 | 0.56 | 0.82 | 1.10 | 1.66 | 2.25 | 3.25 | 4.47 | 54.85 | 52.38 | 75.95 | –79.10 | 1.48×10^4 |

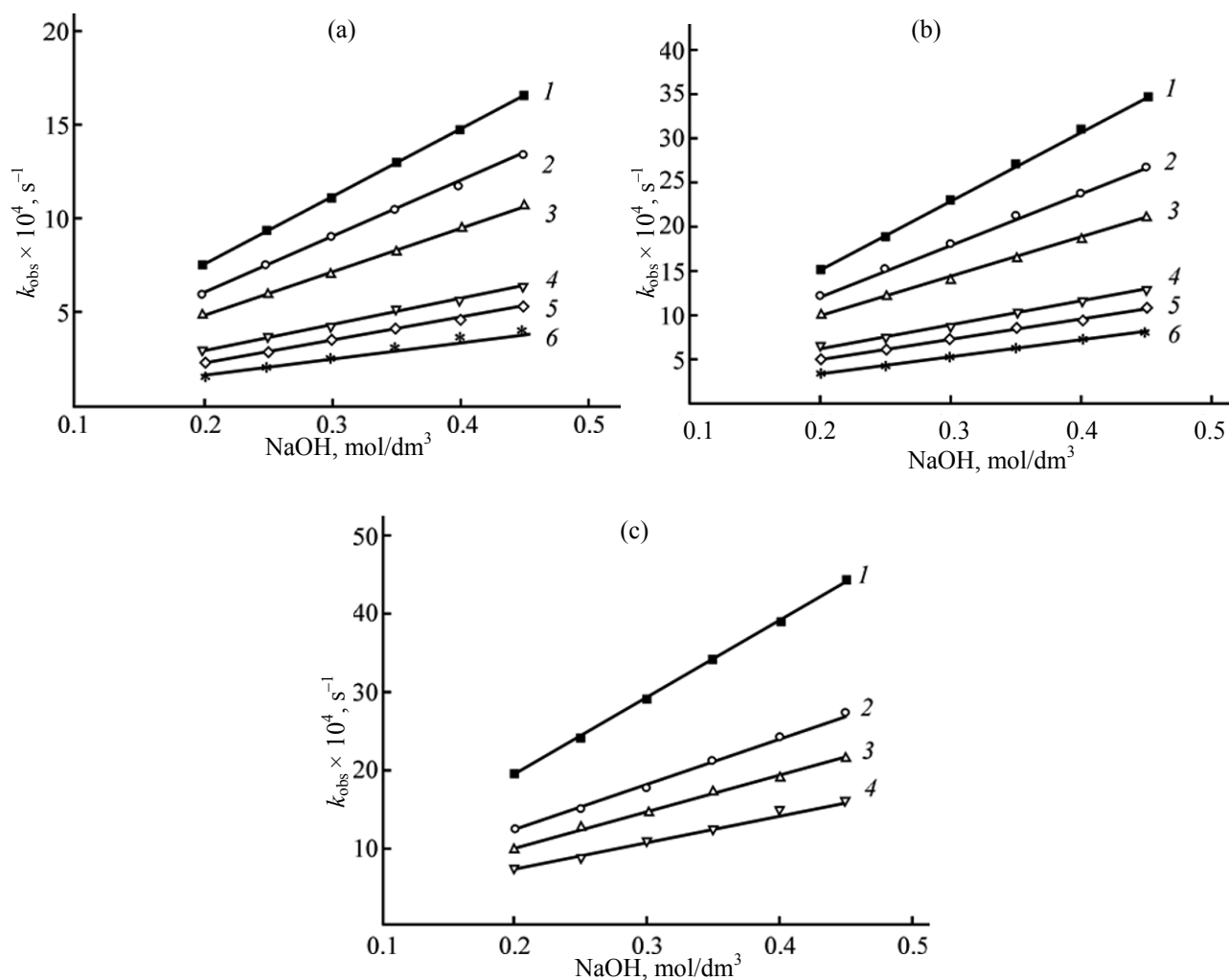


Fig. 2. Plots of the observed first-order rate constants of the base hydrolysis of DMAC in binary methanol–water mixtures versus sodium hydroxide concentration at (a) 288, (b) 298, and (c) 308 K; methanol concentration, vol %: (1) 0, (2) 10, (3) 20, (4) 40, (5) 50, (6) 60.

The observed increase in the second-order rate constant values as the percentage of organic solvent (v/v) in binary mixtures increases can be rationalized by decrease in the concentration of free chromen-2-one derivative due to increase in dispersion forces in solvent molecules. High charge delocalization in DMAC and DEAC molecules promotes interaction with localized dispersion centers in nearby solvent molecules. This interaction is expected to increase in the following order: water < methanol < acetone, and stabilization of the studied compounds changes in the same direction. Furthermore, the transition state is more polar than the initial state, which is consistent with decrease in k_2 values as the fraction of the organic solvent increases.

The higher rate constant values in acetone as compared to methanol may be ascribed to stronger destabilization of hydrophilic OH^- ions in the former solvent [17, 21]. This may also be due to the steric effect related to the size of solvent molecules allowing OH^- ions to pass between larger acetone molecules more readily than between smaller methanol molecules.

The kinetic results conform to Eq. (1):

$$-\partial[\text{substrate}]/\partial \tau = k_2[\text{OH}^-][\text{substrate}]. \quad (1)$$

Here, “substrate” stands for DMAC or DEAC. The dependence of k_{obs} on the base concentration is linear for both DMAC and DEAC without significant intercept (Figs. 2, 3); hence the hydrolysis follows the rate law:

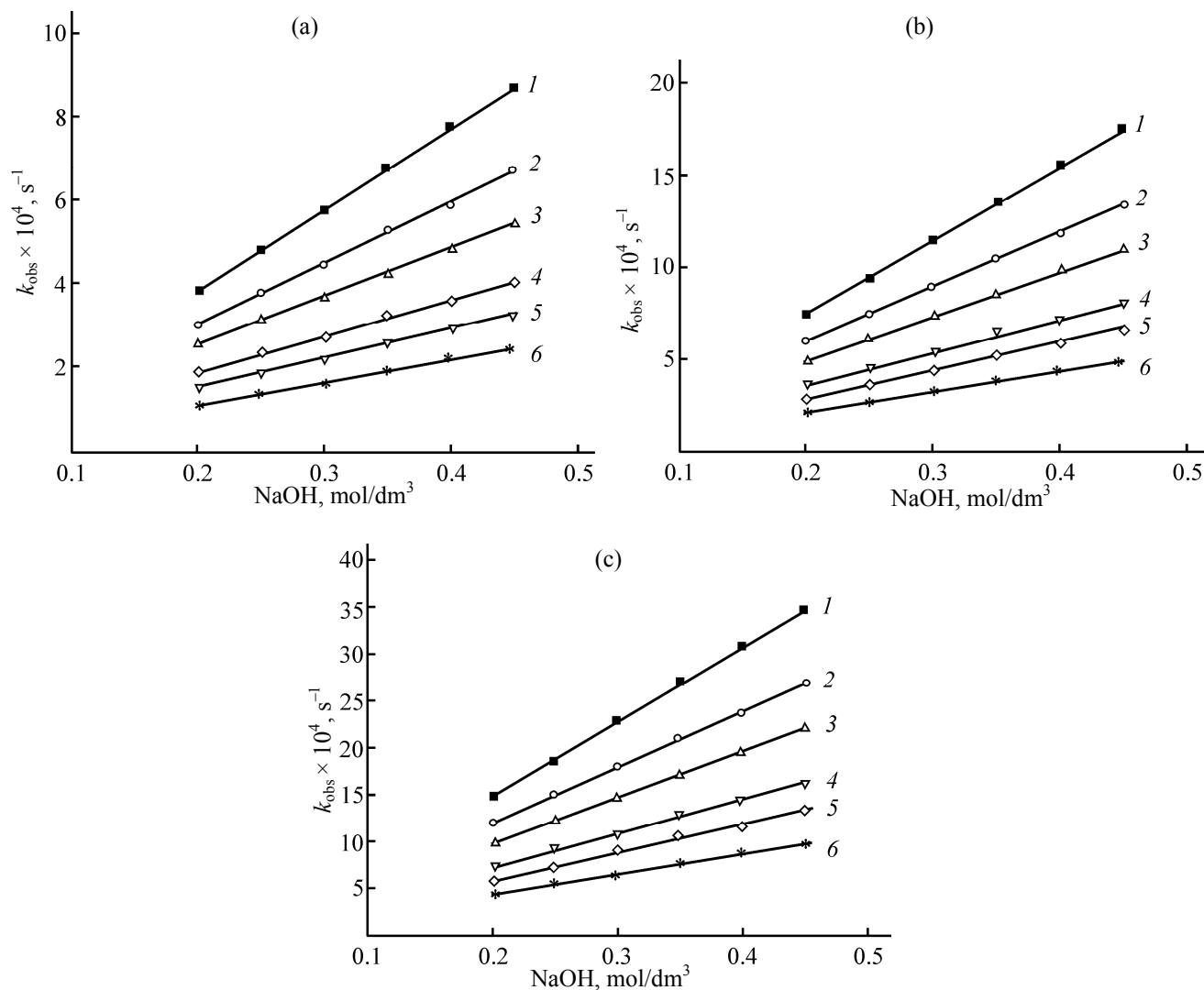


Fig. 3. Plots of the observed first-order rate constants of the base hydrolysis of DEAC in binary methanol–water mixtures versus sodium hydroxide concentration at (a) 288, (b) 298, and (c) 308 K; methanol concentration, vol %: (1) 0, (2) 10, (3) 20, (4) 40, (5) 50, (6) 60.

$$k_{\text{obs}} = k_2[\text{OH}^-], \quad (2)$$

where k_2 is the second-order rate constant provided that $[\text{OH}^-] \gg [\text{substrate}]$. This equation indicates that the second-order process dominates in the examined solvent mixtures.

Tables 1 and 2 show that the observed first-order rate constant of base-catalyzed hydrolysis of DMAC is much greater than the corresponding value for DEAC. This behavior could be attributed to the easier attack by OH^- ion on C^2 in DMAC due to weaker electron-donating ability of the dimethylamino group in DMAC as compared to the diethylamino group in DEAC. This trend is also indicated by the observed decrease in the activation energy for the reaction with DMAC relative

to the corresponding value for the reaction with DEAC.

According to the mechanism proposed for the base hydrolysis of DMAC and DEAC, the following rate equation can be derived by applying the steady-state approximation for the concentration of intermediates **B** and **C**, where the total substrate concentration is given by $[\text{A}]_{\text{T}} = [\text{A}] + [\text{B}] + [\text{C}]$:

$$w = \frac{-\partial[\text{substrate}]}{\partial \tau} = \frac{k_a k_b k_c [\text{OH}^-][\text{A}]_{\text{T}}}{k_a k_b + k_b k_c + k_a k_c [\text{OH}^-]}, \quad (3)$$

$$k_{\text{obs}} = \frac{k_a k_b k_c [\text{OH}^-]}{k_a k_b + k_b k_c + k_a k_c [\text{OH}^-]}. \quad (4)$$

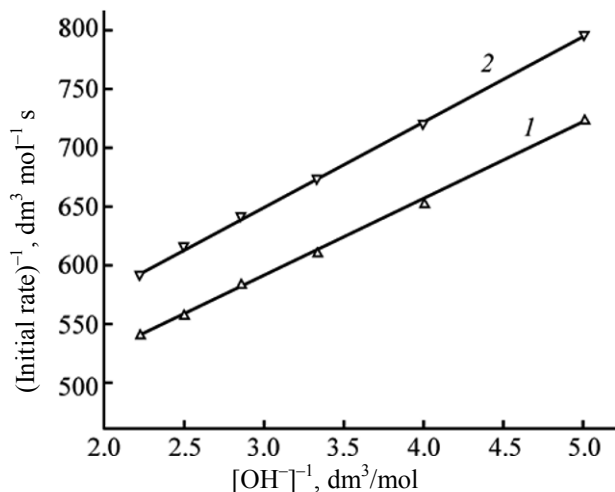


Fig. 4. Lineweaver-Burk plots for the base hydrolysis of (1) DMAC and (2) DEAC in aqueous solution; [substrate] = 1×10^{-7} M, $I = 1.8 \times 10^{-4}$ M, temperature 298 K.

The base hydrolysis of DMAC and DEAC follows Michaelis-Menten kinetics (Fig. 4), i.e., the reaction involves formation of intermediates as shown in Scheme 1. The Michaelis-Menten constants (K_M) were calculated from the Lineweaver-Burk plots and were found to be 0.16 and 0.155 for DMAC and DEAC, respectively. The large values of K_M indicate formation of intermediates during the reaction progress [22–24].

The change in the activation barrier $\delta_m \Delta G^\ddagger$ (Figs. 5, 6) was evaluated from the ratios of the rate constants of the base-catalyzed hydrolysis in aqueous-organic (k_{2S}) to the corresponding values in aqueous solution (k_{2W}) according to Eq. (5) [19, 25]:

$$\delta_m \Delta G^\ddagger = -RT \ln (k_{2S}/k_{2W}). \quad (5)$$

It is worth mentioning that the decrease in the rate constant values of base hydrolysis of DMAC and DEAC as the proportion of methanol or acetone increases is confirmed by the activation parameters. The hydrolysis rate constants are nearly doubled as the temperature increases by 10°C (Figs. 2, 3). The activation parameters were calculated (Tables 1, 2) by the least-squares treatment of the Arrhenius and Eyring plots. The higher energies, enthalpies, free energies, and entropies of activation in methanol relative to the corresponding values in acetone are in agreement with the lower rate constants in methanol as compared to acetone (Tables 1, 2).

The high negative entropies of activation (Tables 1, 2) support the proposed mechanism implying formation of an intermediate complex [17, 24, 26, 27]

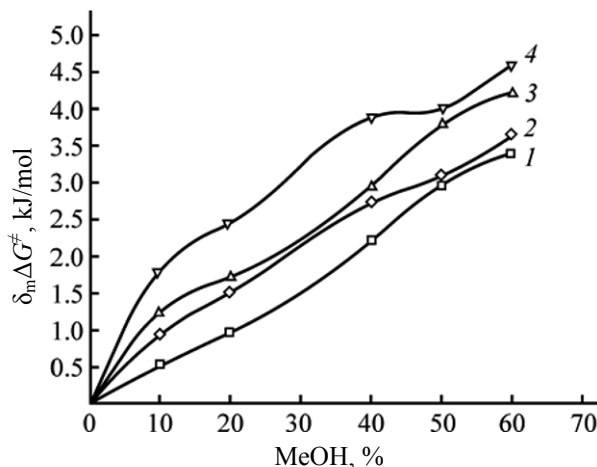


Fig. 5. Plots of the change in the activation barrier ($\delta_m \Delta G^\ddagger$) versus methanol concentration for the base hydrolysis of DMAC in binary methanol-water mixtures at (1) 283, (2) 288, (3) 293, and (4) 298 K.

and indicate rigidity and high stability of complex **B**. This means that the transition state has a more ordered and more rigid structure than the initial reactants [27, 28]. Therefore, ring opening of intermediate complex is likely to be the rate-controlling step which involves inner-sphere electron transfer.

It is interesting that different thermodynamic functions are consistent in their variation trends. Increase in the entropy of activation (ΔS^\ddagger), i.e., its change to less negative values, is accompanied by decrease of the rate constant and increase of the activation energy. This may be due to enhanced stability of the activated complex. Furthermore, the relatively large free energy change suggests that the slow step is ring opening of intermediate **B** and that many vibrational degrees of freedom have been transformed into translations [17, 28, 29]. The large frequency factor provides synergistic evidence for the proposed reaction path. The positive change of the free energy in going from water to methanol or acetone (Figs. 9, 10) assumes that the transient species in hand are polar entities [17, 29].

As seen from Figs. 5 and 6, the change in the activation barrier $\delta_m \Delta G^\ddagger$ decreases with increase in the proportion of methanol or acetone. This trend matches the observed decrease of the second-order rate constants k_2 as the concentration of methanol or acetone increases.

The activation enthalpy (ΔH^\ddagger) and activation entropy (ΔS^\ddagger) are important in controlling the reaction

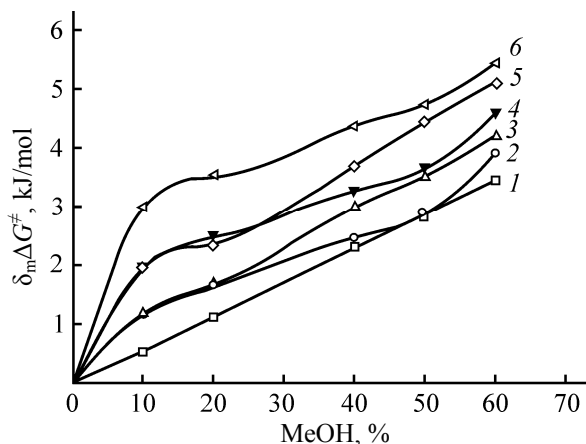


Fig. 6. Plots of the change in the activation barrier ($\delta_m\Delta G^\ddagger$) versus methanol concentration for the base hydrolysis of DEAC in binary methanol–water mixtures at (1) 283, (2) 288, (3) 293, (4) 298, (5) 303 and (6) 308 K.

rate. Plotting of ΔH^\ddagger values against ΔS^\ddagger gives a straight line (Fig. 7). The isokinetic temperature (β) was estimated at 310 K by least-squares treatment of the ΔH^\ddagger – ΔS^\ddagger slope; it exceeded the average experimental temperature ($T_{\text{exp}} = 298$ K) indicating that the reaction is enthalpy-controlled [30, 31]. The straight line obtained suggests that the base-catalyzed hydrolysis reactions of DMAC and DEAC follow a common mechanism with the same rate-determining step.

Thus, the results of our study have shown that base-catalyzed hydrolysis of DMAC and DEAC follows a rate law with $k_{\text{obs}} = k_2[\text{OH}^-]$. The decrease in the rate constants of DMAC and DEAC as the proportion of methanol or acetone increases is due to the destabilization of OH^- ions. The rate constants k_{obs} and k_2 decrease in the following order: water > acetone > methanol. The high negative entropies of activation support the proposed mechanism involving formation of an intermediate complex and suggest rigidity and stability of that complex. Opening of the pyranone ring in the latter is the rate-determining step.

EXPERIMENTAL

All materials, sodium hydroxide (99.3%), sodium chloride (99.7%), sodium nitrate (99%), oxalic acid (99.7%), methanol (99.5%), and acetone (99.5%) were obtained from BDH. 7-Dimethylamino-4-methyl-2H-chromen-2-one and 7-diethylamino-4-methyl-2H-chromen-2-one were obtained from Sigma. Stock solutions of NaOH (1 M), NaCl (1 M), and NaNO_3 (1 M) were prepared by dissolving the calculated

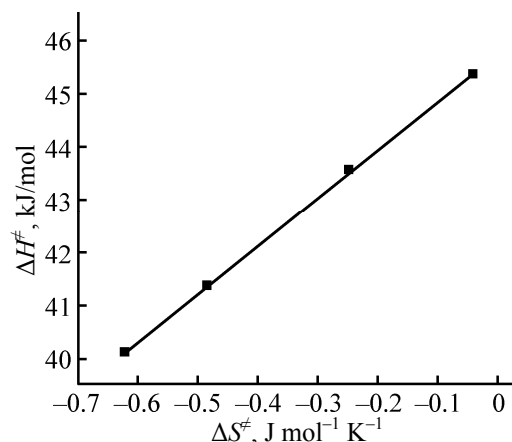


Fig. 7. Isokinetic plot for the hydrolysis of DMAC and DEAC in aqueous solution. The data for HC (7-hydroxy-2H-chromen-2-one) and HCA (7-hydroxy-2-oxo-2H-chromen-4-ylacetic acid) were taken from [17].

amounts of AnalR Normapur® samples in redistilled water.

The kinetics of base-catalyzed hydrolysis were measured by following the dependence of absorbance on time using 10-mm silica cells in a thermostated cell compartment of a JASCO model V-530 spectrophotometer. The reactions were carried out at a constant ionic strength using appropriate amounts of sodium chloride in methanol and sodium nitrate in acetone over at least three half-lives. Pseudofirst-order conditions were applied by mixing multifold greater concentration of NaOH than that of the substrate. The rate constants were calculated from the dependence of absorbance on time at λ 373 nm and 383 nm for DMAC and DEAC, respectively.

The activation parameters were calculated by least-squares treatment of the Arrhenius and Eyring plots. The changes in the activation barrier ($\delta_m\Delta G^\ddagger$) values for DMAC and DEAC in going from water to water–methanol and water–acetone mixtures with various ratios at different temperatures were figured out.

REFERENCES

1. Dall'Acqua, F., Vedaldi, D., and Caffieri, S., *The Fundamental Bases of Phototherapy*, Hönigsmann, H., Jori, G., and Young, A.R., Eds., OEMF, 1996, p. 1.
2. Abu-Eittah, R.H. and El-Tawil, B.A.H., *Can. J. Chem.*, 1985, vol. 63, p. 1173.
3. Kostova, I., *Curr. Med. Chem.: Anti-Cancer Agents*, 2005, vol. 5, p. 29.

4. Kaneko, T., Baba, N., and Matsuo, M., *Chem. Biol. Interact.*, 2003, vol. 142, p. 239.
5. Zacharski, L.R., Wojtukiewicz, M.Z., Constantini, V., Ornstein, D.L., and Memoli, V.A., *Semin. Thromb. Hemost.*, 1992, vol. 18, p. 104.
6. Melagraki, G., Afantitis, A., Markopoulou, O.I., Detsi, A., Koufaki, M., Kontogiorgis, C., and Dimitra, J., *Eur. J. Med. Chem.*, 2009, vol. 44, p. 3020.
7. Christie, R. and Lui, M.H., *Dyes Pigm.*, 1999, vol. 42, p. 85.
8. Chandrashekharan, N. and Kelly, L., *The Spectrum*, 2002, vol. 15, no. 3, p. 1.
9. Camur, M. and Bulut, M., *Dyes Pigm.*, 2008, vol. 77, p. 165.
10. Sokodowska, J., Czajkowski, W., and Podsiadly, R., *Dyes Pigm.*, 2001, vol. 49, p. 187.
11. Egan, D., O'kenedy, R., Moran, E., Cox, D., Prosser, E., and Thornes, D., *Drug Metab. Rev.*, 1990, vol. 22, no. 5, p. 503.
12. Zaprometov, M.N., *Itogi Nauki Tekh., Ser. Biol. Khim.*, 1988, vol. 27, p. 188.
13. Ojala, T., *Biological Screening of Plant Coumarins*, M. Sci. Thesis, University of Helsinki, Finland, 2001.
14. Drexhage, K.H., *Dye Lasers*, Schäfer, F.P., Ed., Berlin: Springer, 1977, 2nd ed.
15. Pavlopoulos, T.G., Boyer, J.H., Politzer, I.R., and Lau, C.N., *Opt. Commun.*, 1987, vol. 64, p. 367.
16. Antonious, M.S. and Sabry, D.Y., *Microchim. Acta*, 1995, vol. 118, p. 69.
17. Abu-Gharib, E.A., El-Khatib, R.M., Nassr, L.A.E., and Abu-Dief, A.M., *J. Korean Chem. Soc.*, 2011, vol. 55, p. 346.
18. Abdel-Mawgoud, A.M., Hamed, M.M., and Mostafa, H.M., *Monatsh. Chem.*, 1997, vol. 128, p. 553.
19. Abu-Gharib, E.A., El-Khatib, R.M., Nassr, L.A.E., and Abu-Dief, A.M., *Z. Phys. Chem.*, 2011, vol. 255, p. 235.
20. Laila H. Abdel-Rahman, Rafat M. El-Khatib, Lobna A. E. Nassr, and Ahmed M. Abu-Dief, *Russ. J. Gen. Chem.*, 2013, vol. 83, no. 12, p. 2510.
21. Blandamer, M.J., Burgess, J., and Roberts, D.L., *J. Chem. Soc., Dalton Trans.*, 1978, p. 1086.
22. Michaelis, L. and Menten, N.L., *Biochem. Z.*, 1918, vol. 49, p. 333.
23. Awad, A.M., Shaker, A.M., Zaki, A.B., and Nassr, L.A.E., *Spectrochim. Acta, Part A*, 2008, vol. 71, p. 921.
24. Nassr, L.A.E., *Int. J. Chem. Kinet.*, 2010, vol. 42, p. 372.
25. Blandamer, M.J., Burgess, J., Clark, B., Duce, P.P., Haken, A.W., Gosal, N., Guradado, P., Sanches, F., Hubbard, C.D., and Abu-Gharib, E.A., *J. Chem. Soc., Faraday Trans. 1*, 1986, vol. 82, p. 1471.
26. Moore, F.M. and Hicks, K.W., *Inorg. Chem.*, 1975, vol. 14, p. 413.
27. Kulkarni, R.M., Bilehal, D.C., and Nandibewoor, S.T., *J. Chem. Res., Synop.*, 2002, p. 147.
28. Jagannadham, V., *Chem.: Bulg. J. Sci. Educ.*, 2009, vol. 18, no. 4, p. 89.
29. El-Khatib, R.M. and Ebaid Nassr, L.A.M., *Spectrochim. Acta, Part A*, 2007, vol. 67, p. 643.
30. Karunakaran, C. and Chidambaranathan, V., *Monatsh. Chem.*, 2000, vol. 131, p. 1123.
31. Karunakaran, C. and Chidambaranathan, V., *Croat. Chem. Acta*, 2001, vol. 74, no. 1, p. 51.